Title

Combining on-line spectroscopy with synchrotron and X-ray free electron laser crystallography.

Authors

Makita, Hiroki
Simon, Philipp
Kern, Jan
et al.

Publication Date

2023-06-01

DOI

10.1016/j.sbi.2023.102604

Peer reviewed

HHS Public Access

Author manuscript

Curr Opin Struct Biol. Author manuscript; available in PMC 2024 January 17.

Published in final edited form as:

Curr Opin Struct Biol. 2023 June ; 80: 102604. doi:10.1016/j.sbi.2023.102604.

Combining on-line spectroscopy with synchrotron and X-ray free electron laser crystallography

Hiroki Makita,

Philipp S. Simon,

Jan Kern,

Junko Yano,

Vittal K. Yachandra

Molecular Biophysics and Integrated Bioimaging Division, Lawrence Berkeley National Laboratory, Berkeley, CA 94720, USA

Abstract

With the recent advances in serial crystallography methods at both synchrotron and X-ray free electron laser sources, more details of intermediate or transient states of the catalytic reactions are being revealed structurally. These structural studies of reaction dynamics drive the need for on-line *In crystallo* spectroscopy methods to complement the crystallography experiment. The recent applications of combined spectroscopy and crystallography methods enable on-line determination of *In crystallo* reaction kinetics and structures of catalytic intermediates, sample integrity, and radiation-induced sample modifications, if any, as well as heterogeneity of crystals from different preparations or sample batches. This review describes different modes of spectroscopy that are combined with the crystallography experiment at both synchrotron and X-ray free-electron laser facilities, and the complementary information that each method can provide to facilitate the structural study of enzyme catalysis and protein dynamics.

Introduction

The mechanism of enzymatic reactions and the associated kinetics are commonly studied using spectroscopic methods in solution, while the structures in the crystalline state are determined with X-ray crystallography, most often using cryo-cooled crystals. The structures of intermediate states are, when possible, determined from crystals that are generated using freeze-quench techniques at different times of the enzymatic reaction. However, most such studies do not use spectroscopy and crystallography simultaneously online, and it is difficult to correlate the structures with the spectroscopic information independently obtained using solution samples. With the advent of X-ray free-electron lasers (XFELs) and the establishment of serial crystallography (SX) over the last five years, it has become possible to determine the structure of intermediate states generated *in situ*. Although such

Corresponding authors: Yachandra, Vittal K (VKYachandra@lbl.gov); Yano, Junko (JYano@lbl.gov); Kern, Jan (JFKern@lbl.gov).

Conflict of interest statement

Nothing declared.

X-ray crystallographic studies provide detailed structural information of enzymes and their active sites, such data alone are insufficient to characterize the reaction kinetics, ligand formation, and oxidation state of the metals in the catalytic site among other key features of protein dynamics. In contrast, different modes of spectroscopy, while unable to generate direct three-dimensional structural information, are capable of clearly identifying such elements of protein dynamics that cannot be attained through X-ray diffraction (XRD) data. Combining structural studies with simultaneous on-line *in situ* spectroscopy, therefore, provides a powerful method to characterize the intermediate states independently. The often complex and multiphasic nature of enzyme catalysis and protein dynamics makes it especially important to establish the reaction timescale and population of the intermediate states (which becomes possible using spectroscopy), that are critical to correctly determine the structures of the intermediate species of interest. Crystallographic data of a transient state often consists of a combination of discrete (meta) stable states that can only be deconvolved accurately with knowledge of the composition of such mixtures. This piece of information can be critically assessed by time-resolved spectroscopy methods. Following this need, several recent crystallography studies have been coupled with spectroscopic characterization of protein samples in both solution and crystal forms. Notably, application of *In crystallo* spectroscopy has been significantly beneficial in determining the enzyme structure, function and reaction kinetics, and mechanism in comparison to those in solution [1–4].

Another important benefit of combined X-ray crystallography and spectroscopy at ambient temperature is the ability to monitor X-ray-induced modification of the sample. The radiation-induced ‘damage’ process involves generation and migration of radicals that affect both the geometric and the electronic structure and has been one of the major challenges in studying metalloenzymes using synchrotron-based X-ray methods [5–7]. While this problem can be partly mitigated by collecting data at cryogenic temperatures and by using several crystals for data collection, it still is a serious limitation for room temperature time-resolved studies. With the advent of XFELs [8], the condition has been changed drastically as the highly intense and ultrafast X-ray pulses generated by XFELs are able to probe the sample on a timescale faster than that of the damage process [9–11]. At ambient temperatures, XFEL is commonly employed in an approach known as serial femtosecond crystallography (SFX) where microcrystals are replaced between each X-ray pulse [12,13]. In this approach, up to hundreds of thousands of crystals are probed to construct a complete diffraction dataset. Combined SFX/spectroscopy experiments make it possible to monitor the integrity of the samples. While larger physical quantities of protein samples are probed in SFX experiments, the ability to closely monitor sample quality such as batch-to-batch homogeneity via simultaneous spectroscopic measurements can improve the quality of these serial experiments.

Given the above described benefits for studies of protein reaction mechanisms and dynamics, as well as the concerns regarding X-ray-induced damage in synchrotron studies and sample quality in serial experiments, different modes of spectroscopy have been combined with the crystallography experiments at both synchrotron and XFEL light sources. Since many enzymes harbor chromophores, characteristic ligand environments, and/or bioinorganic active sites that give rise to distinct spectroscopic signatures, modes of on-line

spectroscopy range from infrared to optical to X-ray, realized using multiple approaches for different purposes. Importantly, tandem measurement of spectra and diffraction from the same sample under identical conditions enable spectroscopy to serve as rapid feedback for crystallography.

Instrumentation

Tandem spectroscopy methods have been applied at synchrotron crystallography beamlines at different light sources, and the most common one is optical absorption microspectroscopy [14–21]. The range of spectroscopy methods extends from absorption, fluorescence, and to Raman spectroscopy, and covers ultraviolet (UV) to near-infrared in spectral ranges. *In crystallo* optical spectroscopy imposes its own challenges over conventional measurement on solution samples [22]. Crystal thickness, high extinction coefficients, concentration of chromophores, and absorption and obstruction by surrounding buffer and the sample mount contribute to difficulties in allowing sufficient light to pass through the sample and to be collected by the detecting optics. The highly scattering nature and limited size of crystalline samples require the probe light to be tightly focused and collection optics to be close to the sample, and in addition, the surroundings of an X-ray interaction point are often congested by devices required for crystallography, which together impose strict geometric constraints.

While constraints are more stringent, several beamlines have adopted a coaxial geometry for optical spectroscopy and X-ray crystallography (Figure 1) [18,19]. Such an alignment is especially beneficial for *in situ* assessment of radiation damage. A collinear configuration enables measurement of the exact same spot on the sample with the same pathlength by the two beams, significantly improving the overlap between optical and X-ray beampaths compared to the off-axis configuration. At SPring-8 BL26B2, two prism mirrors at ~50 mm from the interaction point guide the optical beam through the sample collinear to the X-ray beam [18]. The offset between the two beams is 2° and is designed such that the optical beam avoids the beamstop while retaining the collinearity with the X-rays. At the same time, the prism mounts are designed to only minimally interfere with the diffracted X-rays. The arrangement allows the simultaneous collection of diffraction and spectroscopic data in the on-axis geometry and enables the real-time assessment of radiation damage during irradiation. Furthermore, the spectroscopic system has been installed and operated at the adjacent XFEL facility (SACLA EH4c/BL3), showcasing its adaptability and portability [23].

Combining complementary spectroscopy techniques with XFEL crystallography experiments has a potential for unique X-ray spectroscopy applications. To probe crystal samples using the “diffract before destroy” approach, a fresh sample volume must be delivered to the interaction point before each XFEL pulse. This requirement led to the development of a variety of sample delivery methods [24–28]. These can pose additional challenges for simultaneous spectroscopy due to their more demanding spectroscopic (e.g. scattering density, sample matrix thickness) and geometric requirements. However, because a fresh sample is delivered for each of the femtosecond pulses that are orders of magnitude higher in peak brilliance compared to synchrotron sources, XFELs open the possibility for a series of time-resolved X-ray spectroscopic methods [29,30].

Taking advantage of this capability, simultaneous spectroscopy for XFEL crystallography has been extended to the use of X-ray emission spectroscopy (XES), which is capable of directly assessing the metals in metalloenzyme active sites (Figure 1) [31–33]. An XES spectrum can be generated when the energy of the incoming X-ray beam is above the absorption edge of the element to be detected: this is very advantageous as the same X-ray beam can be used for both XES and crystallography, and also is much more forgiving than for X-ray absorption spectroscopy, where the incident beam needs to be tuned and scanned across the absorption edge energy range. In terms of instrumentation, energy-dispersive analyzer optics are mounted either on a vertical or horizontal plane intersecting the interaction point (orthogonal to the direction of largest elastic scatter which depends on the polarization direction of the XFEL beam), such that the emitted XES signal is diffracted by the analyzers. The diffracted signals are then collected by a position-sensitive detector placed on an opposite plane relative to the analyzers. An advantage of tandem XES and crystallography experiment is that two measurements are taken concurrently using a single probe beam. Hence, sample variability, time lag between crystallography and spectroscopy measurements, beam collinearity, and beam overlap are inherently excluded from being potential issues.

Reaction kinetics for time-resolved crystallography

The advancement in SX methods, both at synchrotron and XFEL sources, has opened the door for a series of time-resolved X-ray diffraction (tr-XRD) studies to capture enzymatic intermediate states and also protein dynamics [34]. Complementary *In crystallo* spectroscopy has been shown highly advantageous for these studies to track the reaction kinetics (which can deviate from solution samples: e.g. the study by Kort et al. [35] and Tosha et al. [36]) and confirm the association of structural dynamics to the reaction segment of interest. The power of the combined methodology is exemplified by a set of recent studies by Aumonier et al., where structural dynamics of the light-oxygen-voltage (LOV) domain of the blue-light photoreceptor phototropin-2 was studied by tr-SX (ESRF ID30A-3 [15]) coupled with time-resolved UV-visible (UV-VIS) absorption spectroscopy (ESRF *ic*OS Laboratory [37]) [38,39]. In these studies, Aumonier et al. surveyed structural dynamics of LOV2 at different delay times following the blue-light illumination, in fast millisecond timescales to capture the buildup of the photoadduct [38], and in slower seconds to minutes timescales to characterize its relaxation process [39]. Optical transient kinetics was essential for determining the population growth rate in the fast phase. Correspondence between the transient kinetics at 390 nm and the rate of changes in the occupancies of the six key residues in LOV2 were used to confirm that the observed structural changes are associated with the photoactivated state conversion.

In the subsequent study where the relaxation process of the photoadduct is monitored, UV-VIS spectroscopy was used to follow the kinetics after the end of blue-light illumination. The comparison of solution and crystal samples exhibits that relaxation kinetics are clearly slowed down *In crystallo*. Following the complete relaxation of the photoactivated chromophores as spectroscopically observed, protein rearrangements involving a crystal phase transition are observed by XRD, with the space group changing from $P4_32_12$ to $P2_12_12_1$ [39]. The study illustrates that the observations from spectroscopy

and crystallography on the same sample and with similar illumination conditions can complement each other as the two techniques are capable of probing different aspect of the protein dynamics, in this case chromophores and protein conformation (Figure 2).

Compared to optical spectroscopy, XES excels in element specificity and therefore can be utilized to track the reaction kinetics of metalloproteins via changes in the oxidation and/or spin state of metal(s) in the active site [40]. In the recent work by Rabe et al., simultaneous tr-SFX and XES was applied to investigate the catalytic reaction of the non-heme iron enzyme isopenicillin N synthase which catalyzes the biosynthesis of the precursor to all natural penicillins [41]. In this work, anaerobic isopenicillin N synthase:-Fe(II):ACV (where ACV is the linear tripeptide substrate) was incubated in oxygen for different exposure times ranging from 400 to 3000 ms prior to detection by an XFEL probe pulse. Structurally, binding of molecular oxygen into the active site and progressive changes in ACV conformation with increasing O_2 exposure time was identified. In the tandem tr-XES measurement, a clear shift in the Fe Kα XES is observed at the time points where O_2 binding is identified by XRD. The direction and magnitude of the shift indicate the change in oxidation state from Fe(II) to Fe(III), supporting the structural observation that the intermediate IPSN:Fe(III):ACV:O_2^- state is present in the 1600–3000 ms timescale (Figure 3) [41].

Similar approaches of combined tr-SFX and XES by XFELs have been applied to a series of metalloenzymes to confirm the structural dynamics in relation to the reaction turn over in metal active. By installing appropriate analyzers, Kα and $K\beta_{1,3}$ XES of Mn, Fe, and Ni in various metalloenzymes have successfully been detected concurrently with XRD [25,41–44]. Furthermore, the configuration of the instrument can be modified to accommodate for multicolor XES measurement in tandem with the tr-SFX, which enables the simultaneous monitoring of systems with multinuclear active sites or heterometallic clusters (Figure 1) [25].

Probe for intermediate state populations and radiation-induced damage/ sample quality

Because of its element sensitivity, parallel XES in tr-SFX experiments has been employed for the purpose of *in situ* and real-time confirmation of sample integrity and homogeneity. Many of the metalloenzymes are highly sensitive not only to radiation dosage but also to sample environment (gas, light, temperature, etc), and as such require careful sample handling to properly trigger and advance the reaction cycle. The oxygen evolving complex in Photosystem II (PS II), which catalytic site consists of a heteronuclear oxo-bridged Mn_4Ca cluster, is one of such highly sensitive systems that require multiple-timed actinic flashes to advance its reaction cycle that catalyzes water oxidation. In a series of XFEL-based tr-SFX studies on PS II, tandem Mn $K\beta_{1,3}$ XES has proven itself to be extremely informative as it was used to confirm (1) Mn XES of the oxygen evolving complex collected by an XFEL pulse indicates no radiation damage [31] and (2) Mn $K\beta_{1,3}$ spectra exhibit a characteristic shift at each metastable state in the reaction cycle due to a collective effect of changes in oxidation states of the four Mn [45]. Additionally, XFEL-based XES on

solution PS II has shown that shifts in spectra at time points between metastable states are in excellent agreement with the reaction rate previously obtained using other time-resolved methods. Moreover, the reaction rate determined by XES coincides with the rate of insertion of additional oxygen into the cluster as determined by XRD (Figure 4) [46].

Due to the larger sample consumption in the SFX approach, oftentimes multiple batches of samples are required for collection of a complete dataset. To monitor the batch-to-batch sample quality through the course of an XFEL experiment, the trend in Mn $K\beta_{1,3}$ in PS II has been utilized to serve as a *in situ* and real-time measure of the batch homogeneity [42]. Live quality control provided by XES is especially critical to the integrity of the tr-SFX experiment. More recently, Mn $K\beta_{1,3}$ XES on crystal and solution PS II obtained using XFELs has been systematically surveyed to investigate the potential effect of the stochastic nature of the XFEL [47]. The study revealed that the spectral effects due to fluctuating pulse intensity and duration are present but negligent in magnitude compared to the spectral shift due to progression of the reaction cycle itself. This finding serves as a key benchmark for the quality-control aspect of XES on metalloenzymes using XFEL.

In synchrotron-based XRD, radiation-induced damages and modifications are more viable concerns. Vergara et al. has demonstrated the application of combined online Raman microspectroscopy and crystallography (SLS X10SA [19]) for the assessment of structural changes induced by irradiation [48]. Using ribonuclease (RNase A) as a model system, the non-resonant Raman shift of RNase A excited by 785 nm light is probed through a course of consecutive XRD measurements. Crystallography data of RNase A sequentially exposed to the X-ray beam displayed a decrease in occupancies of all Met, Asp, and Glu residues. Accordingly, the 522 cm^{-1} band related to the -S-S- mode, the 667 and 724 cm^{-1} bands for -C-S- mode of Met, and the 1410 cm^{-1} band for the $-COO^{-}$ side group of Asp and Glu have all shifted in intensity in the Raman spectra. Following the observation, the authors compiled Raman marker bands to monitor for tracking the radiation damage during the X-ray diffraction data collection.

Similarly, Ishigami et al. recently used coupled UV-VIS microspectroscopy and crystallography at SSRL BL 9–2 to study the effect of radiation dose on the metal site of cytochrome *c* oxidase in its oxidized state [49]. They found that even at 100 K, the metal oxidation state of the active site is rapidly reduced and several features, especially related to the water network in the active site are modified. Interestingly the overall protein structure was observed to be still in the oxidized state. Only after short annealing to above 200 K, a transition of the overall protein to a structure resembling the reduced state was observed, highlighting the importance of parallel spectroscopic measurements especially for metalloenzymes as radiation-induced changes in the metal site might often be subtle and not directly realized when only looking at crystallographic data itself. As in the work by Ishigami et al., optical microspectroscopy has been demonstrated to be a useful tool for tracking radiation-induced metal reduction especially for heme proteins which exhibit characteristic spectral features in the UV-VIS range [17,21]. In a recent survey study by Pfanzagl et al., UV-VIS microspectroscopy at DLS I24 was used to obtain the kinetics of X-ray-induced iron reduction in a diverse set of heme proteins [17]. The rate of photo-reduction was studied on a variety of proteins that differed in iron concentration, number

of ligands, and secondary structural compositions among other aspects. By investigating the photoreduction in a series of systems, they deduced a rate of reduction and a dose limit corresponding to half-maximal reduction at 100 K, both of which were independent of differences in proteins.

Summary and outlook

Combined on-line spectroscopy and crystallography approaches have been explored by multiple synchrotron- and XFEL-based studies to complement the interpretation of structural data on enzymatic reactions and protein dynamics. Major limitations and challenges arise from having access to an appropriate spectrometer at the X-ray beamline, and collecting spectra from a highly scattering crystalline samples of limited volume, within the constraints of the specific delivery method employed. In spite of these difficulties, the applications show that tandem spectroscopy methods serve as powerful tools for determining the reaction kinetics, and as an *in situ* and real-time monitor for radiation-damage and sample quality. Such information is often inaccessible by off-line spectroscopy for highly sensitive samples that require an identical experimental environment, as well as for samples limited in volume. These sets of information are critical in structural studies of enzymatic reaction mechanisms and protein dynamics, especially in tr-SX experiments, which require the accurate determination of the population of intermediate states for the refinement of a mixture of multiple components from the convoluted electron density.

Compared to more mature application in synchrotron-based experiments, the combined approach is still uncommon for XFEL studies. As the application grows, however, it is likely that the available modes of spectroscopy also expands. Flexibility and mobility in design demonstrated by the on-line UV-VIS spectrometer deployed at SPring-8(BL26B2)/SACLA(EH4c/BL3) [18,23] is one promising approach to regularly introduce spectroscopy at other than X-ray wavelengths to the XFEL experiments. The methods established at synchrotron sources, such as UV-VIS absorption, fluorescence, and Raman, are also highly beneficial to the XFEL-based experiments especially for the study of processes that do not involve metal active sites. In addition to incorporation of these synchrotron-tested methods, new tandem approaches will likely cover different modes of X-ray spectroscopy. This effort to expand the modality of combined spectroscopy is demonstrated by a recent work on a simultaneous application of tr-XRD and X-ray absorption spectroscopy on nanoparticles [50].

Acknowledgments

The work from our laboratory was supported by the Director, Office of Science, Office of Basic Energy Sciences, Division of Chemical Sciences, Geosciences, and Biosciences, US Department of Energy [grant number DE-AC02-05CH11231 (to J.Y., V.K.Y., J.K.)]; and the National Institutes of Health [grant numbers GM126289 (to J.K.), GM110501 (to J.Y.), and GM055302 (to V.K.Y.)]. The authors are grateful to our present and former group members and all our collaborators, who contributed to the research from our group presented in this review.

Data availability

No data was used for the research described in the article.

References

Papers of particular interest, published within the period of review, have been highlighted as:

* of special interest

* * of outstanding interest

1. Ronda L, et al. : From protein structure to function via single crystal optical spectroscopy. Front Mol Biosci 2015, 2.
2. Kato Y, et al. : FTIR microspectroscopic analysis of the water oxidation reaction in a single photosystem II microcrystal. J Phys Chem B 2020, 124:121–127. [PubMed: 31825617]
3. Ash PA, et al. : The crystalline state as a dynamic system: IR microspectroscopy under electrochemical control for a [NiFe] hydrogenase. Chem Sci 2021, 12:12959–12970. [PubMed: 34745526]
4. Nomura T, et al. : Short-lived intermediate in N_2O generation by P450 NO reductase captured by time-resolved IR spectroscopy and XFEL crystallography. Proc Natl Acad Sci U S A 2021, 118, e2101481118. [PubMed: 34001620]
5. Yano J, et al. : X-ray damage to the Mn_4Ca complex in single crystals of photosystem II: a case study for metalloprote*In crystallo*graphy. Proc Natl Acad Sci U S A 2005, 102: 12047–12052. [PubMed: 16103362]
6. Holton J: A beginner's guide to radiation damage. J Synchrotron Radiat 2009, 16:133–142. [PubMed: 19240325]
7. Garman EF, Weik M: Radiation damage to biological samples: still a pertinent issue. J Synchrotron Radiat 2021, 28: 1278–1283. [PubMed: 34475277]
8. Emma P, et al. : First lasing and operation of an ångstrom-wavelength free-electron laser. Nat Photonics 2010, 4: 641–647.
9. Chapman HN, Caleman C, Timneanu N: Diffraction before destruction. Philos Trans R Soc B: Biol Sci 2014, 369:20130313.
10. Neutze R, et al. : Potential for biomolecular imaging with femtosecond X-ray pulses. Nature 2000, 406:752–757. [PubMed: 10963603]
11. Chapman HN, et al. : Femtosecond X-ray protein nano-crystallography. Nature 2011, 470:73–77. [PubMed: 21293373]
12. Boutet S, et al. : High-resolution protein structure determination by serial femtosecond crystallography. Science 2012, 337:362–364. [PubMed: 22653729]
13. Barends TRM, et al. : Serial femtosecond crystallography. Nat Rev Methods Primers 2022, 2:59. [PubMed: 36643971]
14. Cohen EA, Doukov T, Soltis SM: UV-visible absorption spectroscopy enhanced X-ray crystallography at synchrotron and X-ray free electron laser sources. Protein Pept Lett 2016, 23: 283–290. [PubMed: 26740326]
15*. von Stetten D, et al. : ID30A-3 (MASSIF-3) - a beamline for macromolecular crystallography at the ESRF with a small intense beam. J Synchrotron Radiat 2020, 27:844–851. [PubMed: 32381789] An overview of a synchrotron-based crystallography beamline with an integrated on-line In crystallo optical microspectrophotometer. Applications of the beamline and the spectrometer are showcased in the work by Aumonier et al.
16. von Stetten D, et al. : Online Raman spectroscopy for structural biology on beamline ID29 of the ESRF. J Struct Biol 2017, 200: 124–127. [PubMed: 29042242]
17**. Pfanzagl V, et al. : X-ray–induced photoreduction of heme metal centers rapidly induces active-site perturbations in a protein-independent manner. J Biol Chem 2020, 295:13488–13501. [PubMed: 32723869] A survey work on X-ray induced reduction kinetics of a series of heme proteins with combined UV-VIS microspectroscopy. The set of proteins studied in this work covers different iron content per unit, different number of coordination to the heme group, a variety of secondary structure compositions, as well as different crystal morphologies. By using UV-VIS signal to track the radiation damage, they found that the photoradiation kinetics is

independent of differences in proteins, and proposed a dose limit for cryotemperature that is sufficient for 50% and 5% reduction.

18. Sakaguchi M, et al. : A nearly on-axis spectroscopic system for simultaneously measuring UV-visible absorption and X-ray diffraction in the SPring-8 structural genomics beamline. J Synchrotron Radiat 2016, 23:334–338. [PubMed: 26698082]
19. Pompidor G, et al. : A new on-axis micro-spectrophotometer for combining Raman, fluorescence and UV/Vis absorption spectroscopy with macromolecular crystallography at the Swiss Light Source. J Synchrotron Radiat 2013, 20:765–776. [PubMed: 23955041]
20. Orville AM, et al. : Correlated single-crystal electronic absorption spectroscopy and X-ray crystallography at NSLS beam-line X26-C. J Synchrotron Radiat 2011, 18:358–366. [PubMed: 21525643]
21. Zárate-Romero A, et al. : X-ray driven reduction of Cpd I of Catalase-3 from N. crassa reveals differential sensitivity of active sites and formation of ferrous state. Arch Biochem Biophys 2019, 666:107–115. [PubMed: 30940570]
22. Dworkowski FSN, et al. : Challenges and solutions for the analysis of *in situ*, *In crystallo* micro-spectrophotometric data. Acta Crystallogr D 2015, 71:27–35. [PubMed: 25615857]
23. Shimada A, et al. : A nanosecond time-resolved XFEL analysis of structural changes associated with CO release from cytochrome c oxidase. Sci Adv 2017, 3:e1603042. [PubMed: 28740863]
24. Srinivasan M, et al. : Recent advances and future prospects of serial crystallography using XFEL and synchrotron X-ray sources. Biodesign 2015, 3:98–110.
25. Fuller FD, et al. : Drop-on-demand sample delivery for studying biocatalysts in action at X-ray free-electron lasers. Nat Methods 2017, 14:443–449. [PubMed: 28250468]
26. Zhao F-Z, et al. : A guide to sample delivery systems for serial crystallography. FEBS J 2019, 286:4402–4417. [PubMed: 31618529]
27. Cheng RK: Towards an optimal sample delivery method for serial crystallography at XFEL. Crystals 2020:10, 10.3390/cryst10030215.
28. Orville AM: Recent results in time resolved serial femtosecond crystallography at XFELs. Curr Opin Struct Biol 2020, 65:193–208. [PubMed: 33049498]
29. Bergmann U, et al. : Using X-ray free-electron lasers for spectroscopy of molecular catalysts and metalloenzymes. Nat Rev Phys 2021, 3:264–282. [PubMed: 34212130]
30. Alonso-Mori R, et al. : Energy-dispersive X-ray emission spectroscopy using an X-ray free-electron laser in a shot-by-shot mode. Proc Natl Acad Sci U S A 2012, 109:19103–19107. [PubMed: 23129631]
31. Kern J, et al. : Simultaneous femtosecond X-ray spectroscopy and diffraction of photosystem II at room temperature. Science 2013, 340:491–495. [PubMed: 23413188]
32. Kern J, et al. : Taking snapshots of photosynthetic water oxidation using femtosecond X-ray diffraction and spectroscopy. Nat Commun 2014, 5:4371. [PubMed: 25006873]
33. Kern J, Yachandra VK, Yano J: Metalloprotein structures at ambient conditions and in real-time: biological crystallography and spectroscopy using X-ray free electron lasers. Curr Opin Struct Biol 2015, 34:87–98. [PubMed: 26342144]
34. Brändén G, Neutze R: Advances and challenges in time-resolved macromolecular crystallography. Science 2021, 373.
35. Kort R, et al. : Characterization of photocycle intermediates in crystalline photoactive yellow protein. Photochem Photobiol 2003, 78:131–137. [PubMed: 12945580]
36. Tosha T, et al. : Capturing an initial intermediate during the P450nor enzymatic reaction using time-resolved XFEL crystallography and caged-substrate. Nat Commun 2017, 8:1585. [PubMed: 29147002]
37. von Stetten D, et al. : *In crystallo* optical spectroscopy (icOS) as a complementary tool on the macromolecular crystallography beamlines of the ESRF. Acta Crystallogr D 2015, 71:15–26. [PubMed: 25615856]
38*. Aumonier S, et al. : Millisecond time-resolved serial oscillation crystallography of a blue-light photoreceptor at a synchrotron. IUCrJ 2020, 7:728–736.A combined synchrotron-based tr-XRD and UV-visible spectroscopy study tracking the structural and spectroscopic changes of a blue-

light photoreceptor on a millisecond timescale. Tandem transient optical spectroscopy is applied to adjust the illumination condition such that the resulting kinetics are on a preferred timescale.

39**. Aumonier S, et al. : Slow protein dynamics probed by time-resolved oscillation crystallography at room temperature. IUCrJ 2022, 9:756–767.A second study in series by the same group using the combined tr-XRD and optical In crystallo spectroscopy using the synchrotron source. In this study, slower protein dynamics in the second to minute timescales is investigated. In crystallo spectroscopy reveals the kinetics of photoadduct relaxation is considerably slower in a crystal sample than in solution form. The relaxation kinetics as determined by optical spectroscopy and the rate of disappearance of photoadduct-forming conformer observed through crystallography show excellent agreement. Additionally, much slower structural changes that is independent of adduct formation/relaxation is observed.

40. Bergmann U, Glatzel P: X-ray emission spectroscopy. Photosynth Res 2009, 102:255–266. [PubMed: 19705296]

41**. Rabe P, et al. : X-ray free-electron laser studies reveal correlated motion during isopenicillin N synthase catalysis. Sci Adv 2021, 7.An XFEL-based simultaneous tr-SFX and XES study on IPNS. Redox state of an iron in the active site at different O2 exposure time is monitored by XES, concurrently with structural changes. The combined study identified that a superoxide intermediate is formed during the catalysis. XRD data shows the binding of molecular oxygen in the vicinity of the iron, and XES shows a shift in Fe Kα spectrum that is correlated in timing with the appearance of O2 in the binding site.

42. Fransson T, et al. : X-ray emission spectroscopy as an *in situ* diagnostic tool for X-ray crystallography of metalloproteins using an X-ray free-electron laser. Biochemistry 2018, 57: 4629–4637. [PubMed: 29906115]

43. Srinivas V, et al. : High-resolution XFEL structure of the soluble methane monooxygenase hydroxylase complex with its regulatory component at ambient temperature in two oxidation states. J Am Chem Soc 2020, 142:14249–14266. [PubMed: 32683863]

44. Ohmer CJ, et al. : XFEL serial crystallography reveals the room temperature structure of methyl-coenzyme M reductase. J Inorg Biochem 2022:230.

45. Kern J, et al. : Structures of the intermediates of Kok's photosynthetic water oxidation clock. Nature 2018, 563: 421–425. [PubMed: 30405241]

46**. Ibrahim M, et al. : Untangling the sequence of events during the S(2)–> S(3) transition in photosystem II and implications for the water oxidation mechanism. Proc Natl Acad Sci U S A 2020, 117:12624–12635. [PubMed: 32434915] The paper applies simultaneous tr-SFX and Mn Kβ1,3 XES to study the geometric and electronic transitions in the oxygen-evolving complex in photosystem II at room temperature. Catalytic reaction is advanced using multiple timed visible light flashes and XRD data are collected at multiple time points to construct a "molecular movie". A series of molecular movements leading to an insertion of a new bridging oxygen ligand is identified through XRD, and the XES trend shows a shift in Mn oxidation that correlates with the appearance of the new oxygen in the Mn4Ca cluster.

47*. Fransson T, et al. : Effects of x-ray free-electron laser pulse intensity on the Mn Kβ1,3 x-ray emission spectrum in photosystem II—a case study for metalloprotein crystals and solutions. Struct Dyn 2021, 8:64302.A survey study of Mn $K\beta_{1,3}$ XES of oxygen-evolving complex in photosystem II using XFELs. The potential effects of intense and stochastic XFEL pulses on the XES signal is investigated. Both the microcrystal and solution samples are surveyed.

48. Vergara A, Caterino M, Merlino A: Raman-markers of X-ray radiation damage of proteins. Int J Biol Macromol 2018, 111: 1194–1205. [PubMed: 29374529]

49**. Ishigami I, et al. : Temperature-dependent structural transition following X-ray-induced metal center reduction in oxidized cytochrome c oxidase. J Biol Chem 2022, 298.A detailed study of the redox state of the metal site in cytochrome c oxidase using combined UV-VIS and crystallography showing that the metal center is rapidly reduced by X-rays, leading to localized structural changes especially in the water network, but with the overall protein environment being locked in the oxidized state.

50. Lützenkirchen-Hecht D, et al. : Simultaneous quick-scanning X-ray absorption spectroscopy and X-ray diffraction. J Phys Conf Ser 2022, 2380.

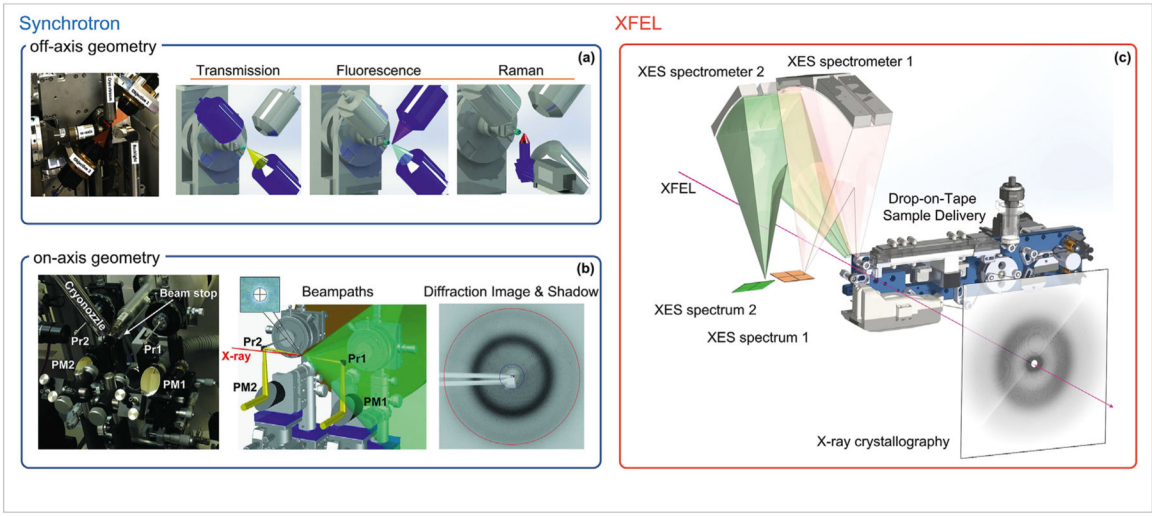

Figure 1.

Configurations for on-line spectroscopy setup at X-ray crystallography beamlines. **(a)** Experimental setup of an off-axis micro-spectrophotometer at a synchrotron beamline (ESRF ID30A-3 [15]), and configurations of objective lenses for different modes of spectroscopy (ESRF ID29 [37]). The off-axis configuration is more flexible and enables transmission, fluorescence, and Raman spectroscopy with minimal changes in the arrangement. Figures adapted from Refs. [15,37]. **(b)** Experimental setup for on-axis transmission spectroscopy at a synchrotron source (SPring-8 BL26B2 [18]). Using the on-axis configuration, the same sample spot with the same pathlength can be probed by X-ray and optical beams. This type of arrangement therefore enables highly accurate assessment of radiation-induced damage. In the specific configuration depicted here, X-ray and optical beam paths (in red and yellow, respectively) are slightly offset from each other such that the optical components do not interfere with the XRD data collection. As such, XRD and UV-visible measurements can be taken concurrently. Figure adapted from Ref. [18]. **(c)** Schematic of simultaneous XRD and XES experiment at XFEL sources using the Drop-on-Tape sample delivery system. The setup utilizes one or two sets of von Hamos spectrometers for XES data collection, which enables the detection of emission spectra on a shot-by-shot basis. By installing appropriate analyzer crystals on the spectrometers, different combinations of Kα and $K\beta_{1,3}$ XES of Mn, Fe, and Ni have been obtained concurrently with the XRD data [25,41,43,44,46]. XES, X-ray emission spectroscopy; XFEL, X-ray free electron laser; XRD, X-ray diffraction.

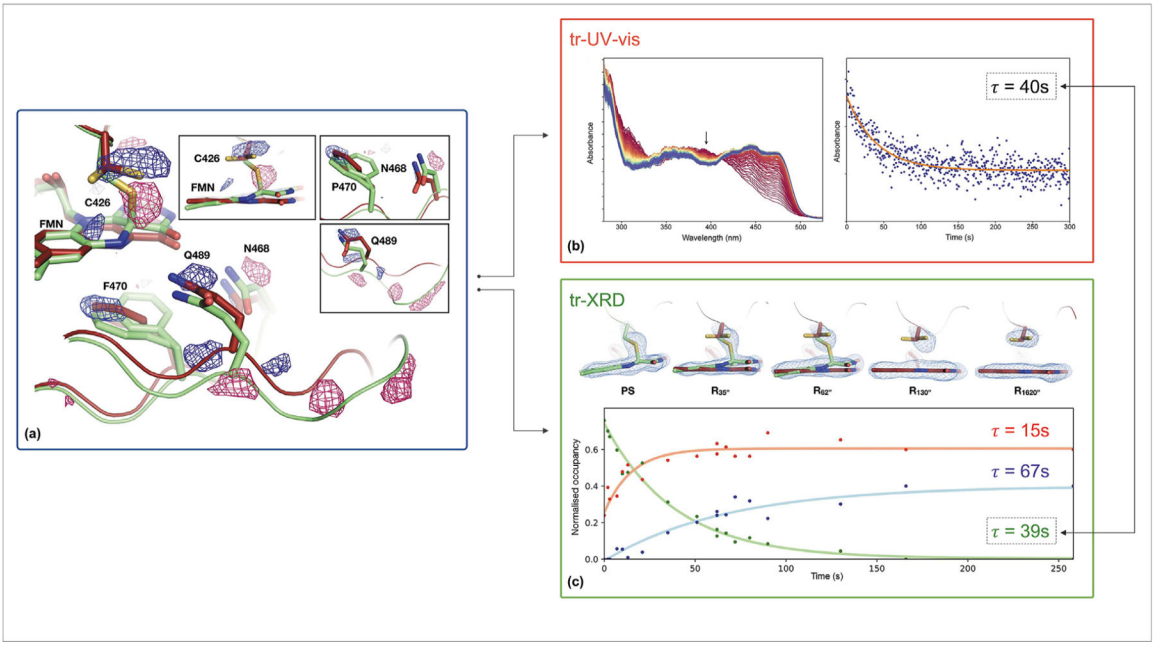

Figure 2.

Combined time-resolved XRD and UV-visible spectroscopy study of the LOV2 domain [39]. Relaxation of the photoadduct in the seconds timescale is studied at room temperature using a synchrotron source with tandem *In crystallo* spectroscopy. **(a)** Structural rearrangements around flavin mono-nucleotide (FMN) as depicted by Fourier difference maps calculated between the photostationary state (continuously illuminated state) and 35s into relaxation in the dark. Positive and negatives peaks are shown as blue and pink meshes, respectively. The green model is the L-state, one of the photostationary conformations, and the red model is the D″-state, a state that the photostationary equilibrium state relaxes into after a prolonged period in the dark. **(b)** Evolution of UV-visible spectra of a LOV2 crystal during the relaxation of the photoadduct. A slice of spectrum is recorded every 500 ms for 300 s after the end of blue-light illumination. Early and late timepoints are shown as red and blue spectra, respectively. The absorption peak at 390 nm is marked to denote the characteristic band of the LOV2 L-state. The decay of this 390 nm absorbance was monitored over time, and a relaxation time constant of 40 s was obtained. This time constant is considerably slower than a time constant of 6 s found for the solution sample in the same setup, and signifies the importance of complementary *In crystallo* spectroscopy in the tr-XRD studies. **(c)** Relaxation of the photoadduct as monitored by tr-XRD. The top panel shows the evolution of the $2F_o$-F_c map around the C426 side chain (which forms the photoadduct) and the FMN at select time points. The bottom panel shows the occupancy level of the three conformers of C426. The green conformation is the photoadduct conformation, and its rate of disappearance agrees exceptionally well with the rate constant of relaxation determined by the spectroscopic signature in **(b)**. Orange and blue are two ground state conformations that are formed as a result of relaxation. Figure adapted from the study by Aumonier et al. [39]. LOV, light-oxygen-voltage; UV, ultraviolet; XRD, X-ray diffraction.

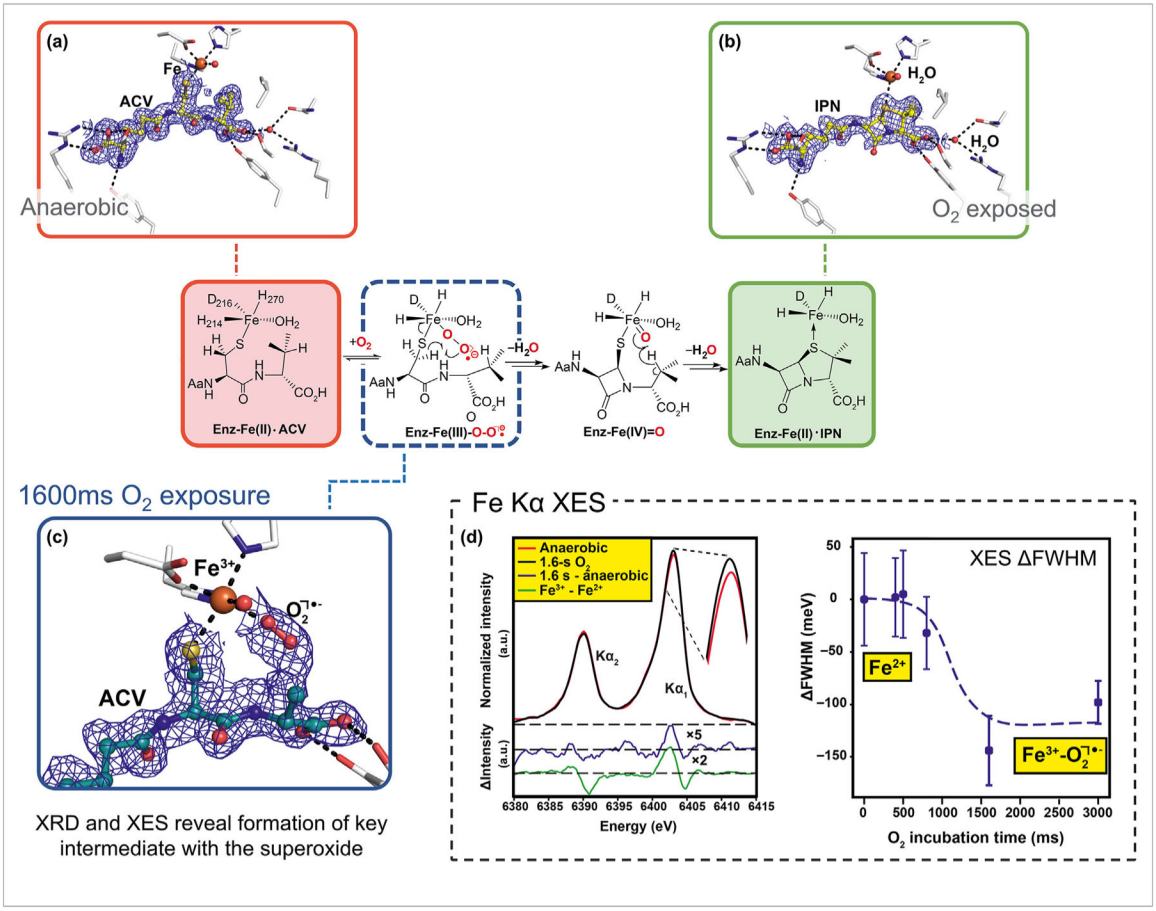

Figure 3.

Combined tr-SFX and XES study of IPNS by XFEL [41]. $2mF_o$-DF_c composit omit electron density map for **(a)** anaerobic IPNS:Fe:ACV and **(b)** for IPNS:Fe:IPN obtained by exposing IPNS:Fe:ACV microcrystals to O_2 for ~30 min. **(c)** $2mF_o$-DF_c map of the IPNS:Fe^{3+}:ACV:$O_2^{\bullet-}$ complex obtained after 1600 ms O_2 exposure of anaerobic IPNS:Fe:ACV microcrystals. Positive electron density that appeared at the Fe coordination site is best fitted by binding of molecular oxygen “end-on” to the Fe. **(d)** Fe Kα XES of anaerobic (red) and 1600 ms O_2-exposed (black) IPNS:Fe:ACV microcrystals. A difference spectrum (blue) compares well with a difference signal of 10 mM Fe(III)Cl_3 and Fe(II)Cl_2 solutions, and indicates a similar change in the oxidation state. The full width at half maximum (FWHM) of the Fe $Kα_1$ peak following O_2 exposure shows relatively small changes at early time points, but a shift of ~0.1 eV at 1600 ms and 3000 ms time points. The difference spectrum and changes in FWHM both indicate a change in Fe oxidation at around 1600 ms, which supports the appearance of electron density in the vicinity of Fe in the active site. Figure adapted from the study by Rabe et al. [41]. IPNS, isopenicillin N synthase; SFX, serial femtosecond crystallography; XES, X-ray emission spectroscopy; XFEL, X-ray free electron laser.

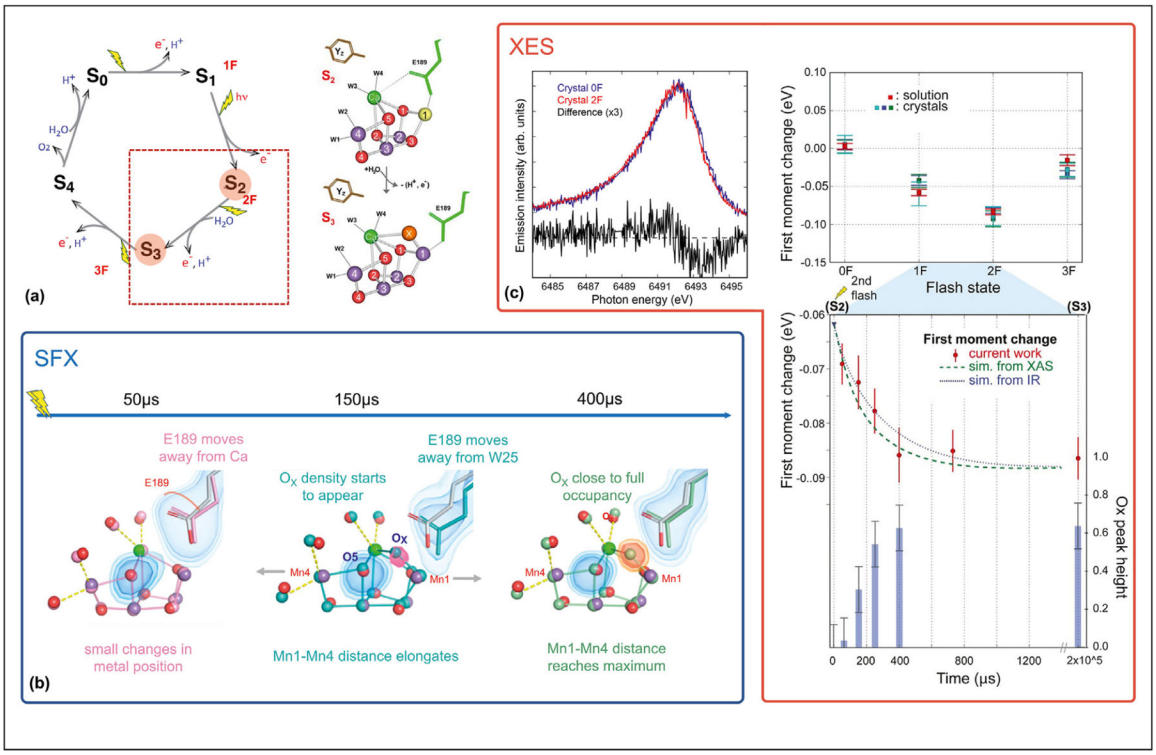

Figure 4.

XFEL-based simultaneous tr-SFX and XES study of the OEC in PS II [46]. **(a)** Kok cycle of the water oxidation reaction describing the different metastable intermediate states triggered by actinic flashes. The structures of the Mn_4Ca cluster show the major changes between the S_2 and S_3 states (O: red, Ca^{2+}: green, Mn^{3+}: yellow, Mn^{4+}: purple). **(b)** F_o-F_C electron density omit maps detailing structural changes at the OEC in the $S_2 \rightarrow S_3$ transition. D1-E189 (blue), O5 (blue), and O_X (red) are separately omitted to construct the map. E189 starts to shift at 50 ms, and makes more pronounced movement by 150 ms. The O_X density starts to appear at 150 ms and is accompanied by elongation of the Mn1–Mn4 distance. At 400 ms, the O_X density is close to full occupancy and the Mn1–Mn4 distance reaches maximum separation. **(c)** Mn $K\beta_{1,3}$ XES of PS II microcrystals, in the S_1 state (0 flash, blue) and the S_3 state (2 flashes, red), and its difference spectrum. The first moment of the metastable states shifts toward lower energy in response to the first two flashes, and to higher energy in the third flash (top panel). During the $S_2 \rightarrow S_3$ transition, the change in first moment follows a similar rate as the rates predicted by separate XAS and IR studies. Moreover, the rate of Mn oxidation as observed via XES agrees well with the rate of increase in the O_X omit density. Figure adapted from the study by Ibrahim et al. [46].

XAS, X-ray absorption spectroscopy; XES, X-ray emission spectroscopy; XFEL, X-ray free electron laser; SFX, serial femtosecond crystallography.